Available online at www.sciencedirect.com
ScienceDirect
Mendeleev Commun., 2019, **29**, 309–311

Mendeleev Communications

Superoxide-assisted electrochemical deposition of semiconductor polyhydroxyphenylporphyrin films

Sergey M. Kuzmin,*[a,b] Svetlana A. Chulovskaya,[a] Vladimir I. Parfenyuk[a,c] and Oskar I. Koifman[c]

[a] *G. A. Krestov Institute of Solution Chemistry, Russian Academy of Sciences, 153045 Ivanovo, Russian Federation. E-mail: smk@isc-ras.ru*
[b] *Ivanovo State Power Engineering University, 153003 Ivanovo, Russian Federation*
[c] *Ivanovo State University of Chemistry and Technology, 153000 Ivanovo, Russian Federation*

DOI: 10.1016/j.mencom.2019.05.023

The method of superoxide-assisted electrochemical deposition was employed for the formation of film materials based on hydroxyphenylporphyrins and their metal complexes. The C–O–C bridges were the major moieties for bonding porphyrins inside the electropolymer. The obtained polyporphyrin films demonstrated a hole type of conductivity, which makes them suitable for various applications.

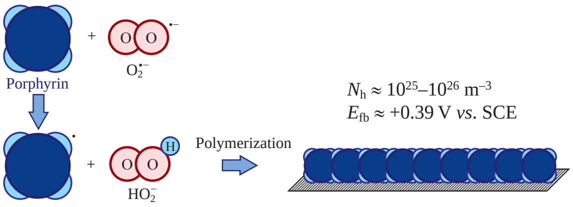

Porphyrin-based film materials are widely applied in the design of a number of functional devices.[1–5] Films of hydroxyphenyl porphyrin are useful as sensors,[6,7] nonlinear optical materials,[8] organic ferroelectrics,[9] electrocatalysts,[10] and fluorescent materials in organic light-emitting diodes.[11] We have recently demonstrated that aminophenyl porphyrins allow one to produce functional films from DMSO solutions by the new superoxide-assisted electrochemical deposition method.[12,13] It has been supposed that this method can be successfully used for the formation of functional films of hydroxyphenyl porphyrins *via* the interaction between hydroxyphenyl porphyrins and superoxide generating porphyrins bearing a reactive phenoxyl radical as the substitutent according to other[14,15] and our[16–20] previous reports. In this work, we have shown that polymer films of hydroxyphenyl porphyrins can be produced *via* the superoxide-assisted electrochemical deposition and verified semiconductor properties of the obtained films.

5,10,15,20-Tetrakis(3-hydroxyphenyl)porphyrin **1**, 5,10,15,20-tetrakis(4-hydroxyphenyl)porphyrin **2**, and their zinc complexes **3** and **4** were obtained *via* the known two-step procedure[21,22] and their characteristics were consistent with those reported earlier.[23,24]

Electrooxidation and electroreduction of hydroxyphenyl porphyrins studied using compound **2** in degassed DMSO solutions [Figure 1(*a*), curve *2*] are irreversible processes without significant changes in the electrochemical responses from cycle to cycle. No film formation on the working electrode was observed. In the absence of porphyrin [see Figure 1(*a*), curve *3*], oxygen electroreduction in DMSO is quasi-reversible and proceeds *via* a one-electron mechanism resulting in superoxide ($O_2^{\bullet -}$) formation: $O_2 + e \rightarrow O_2^{\bullet -}$.[25,26] The oxygen electroreduction becomes irreversible in oxygen-saturated solutions of hydroxyphenyl porphyrin. We have also observed a change in the CV curve shape from cycle to cycle [see Figure 1(*a*), curve *4*] and formation of a film on the surface of the working electrode.

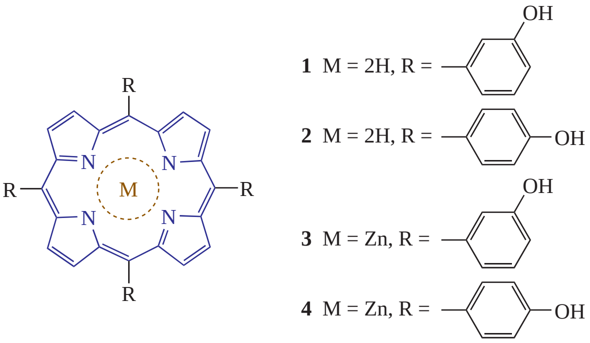

1 M = 2H, R =
2 M = 2H, R =
3 M = Zn, R =
4 M = Zn, R =

The data obtained by the electrochemical quartz microbalance (EQMB) method under natural aeration conditions revealed that the electrodeposition of investigated hydroxyphenyl porphyrins is similar to compound **2**, with some variations in the intensity and position of the desorption waves and difference in the contribution of direct porphyrin electroreduction during the film formation. After 20 cycles, the masses of the film on the working electrode were: 2.15, 1.85, 2.40, and 1.73 μg for compounds **1**–**4**, respectively. There were two waves of poly-**2** film mass increase in the cathode region for the first cycle [Figure 1(*b*)]. The film formation began at the potential of onset of oxygen electroreduction. The second wave of film deposition indicates that the porphyrin anion was involved in the polymerization process probably due to its interaction with $O_2^{\bullet -}$ or dissolved oxygen. The film deposition associated with the porphyrin electrooxidation process as well as the film desorption were observed in the anodic region. The significant film growth was noted after the potential passed through the range of oxygen electroreduction, both in the forward and reverse directions, starting from the second cycle. The desorption and deposition waves were shifted towards positive potentials during the potential cycling and film formation [see Figure 1(*b*)]. Consequently, no film deposition was detected due to the direct porphyrin electrooxidation after the third cycle. Beginning from the fifth cycle, the formation of poly-**2** films appeared as a broad wave once the potential passed through the range of oxygen electroreduction. Thus, the film formation process involves an interaction of hydroxyphenyl porphyrins with superoxide to give porphyrins bearing a reactive phenoxyl

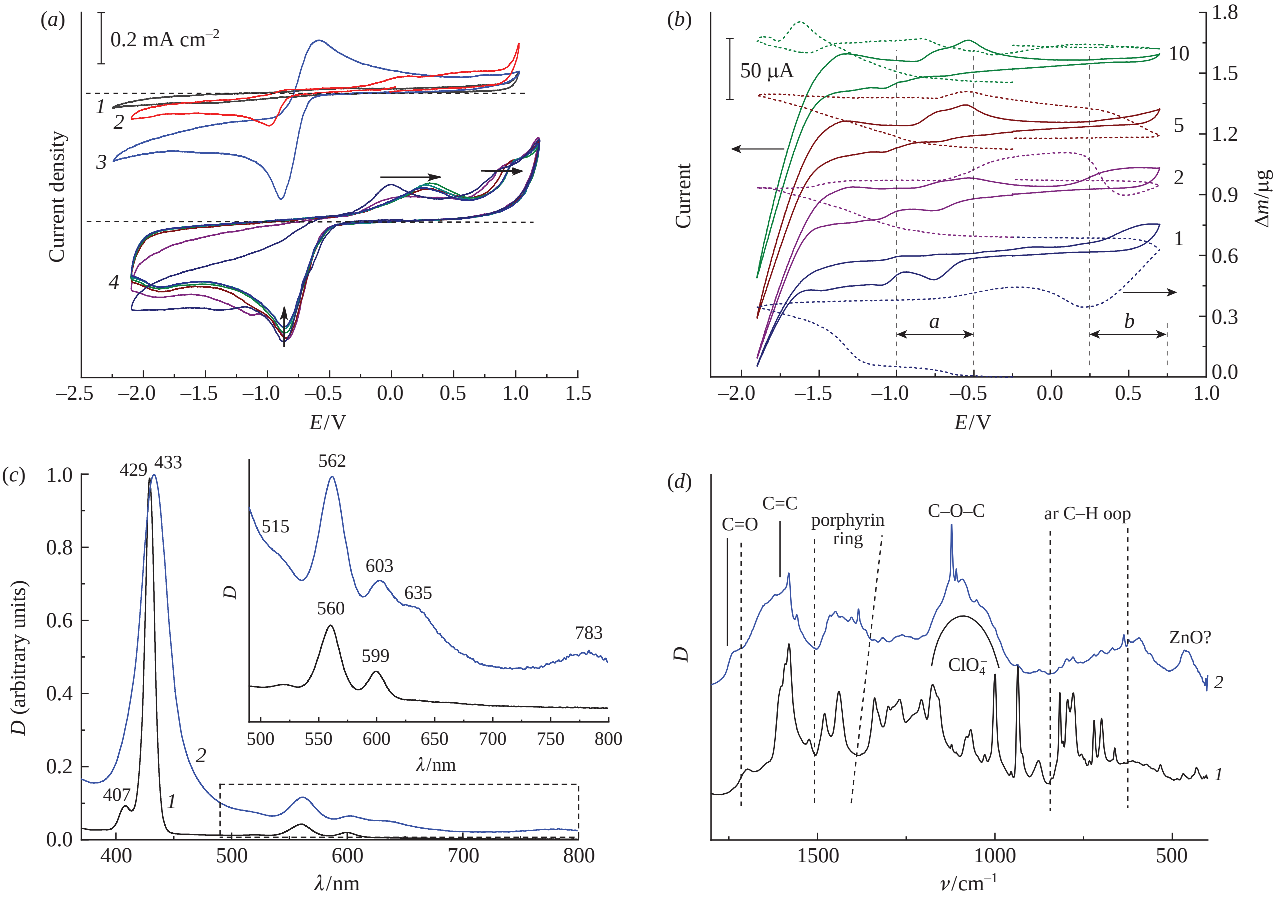

Figure 1 (*a*) Electrochemical responses in DMSO on glassy carbon electrode of (*1*) background current, (*2*) **2** in a degassed solution, (*3*) oxygen in DMSO without porphyrin, and (*4*) **2** in an oxygen-saturated solution. The tendency of the CV curve change is shown by arrows, the scan rate was 0.02 V s^{-1}. (*b*) EQCM data on the deposition of **2** on Pt in an air saturated DMSO. The potentials were measured *vs*. Ag/AgCl electrode, the scan rate was 0.02 V s^{-1}. The numbers 1, 2, 5, and 10 correspond to the number of cycle, '*a*' is the range of oxygen electroreduction, and '*b*' is the range of porphyrin electrooxidation. (*c*) UV-VIS spectra of **3** in (*1*) a DMSO solution and (*2*) in a film on an ITO electrode. The range of Q-band (*D* × 10) is shown in the inset. (*d*) A fragment of the vibrational spectra of (*1*) compound **3** and (*2*) poly-**3** films.

radical as a substituent and then triggering a radical-chain mechanism for the formation of a polymer film. This mechanism may include a dehydrogenative coupling of phenoxyl radicals with aryl moieties of another porphyrin molecule resulting in the formation of C–O–C bridges. This was assumed taking into account the recent report[27] on the aromatic substrates functionalization.

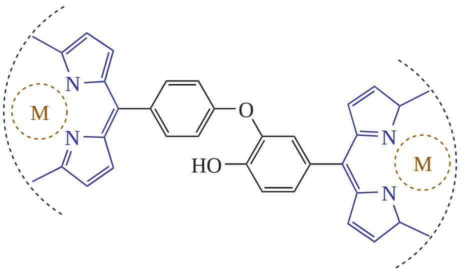

Spectral data have confirmed the EQMB results. The spectral characteristics of the precursor and resulting film [Figure 1(*c*),(*d*)] were compared using compound **3** as the example. The presence of Soret (433 nm) and Q (562 and 603 nm) bands in the spectrum of poly-**3** films indicates that the inner Zn ion is preserved in the undestroyed porphyrin core during electropolymerization. The red shift of the Soret band and its broadening are typical of porphyrins in the polymerized state with the preserved structure of the porphyrin core.[28] The appearance of absorption bands near 515 and 635 nm apparently points out the presence of porphyrin-quinoid fragments.[29] The appearance of band with maximum at 783 nm may be explained by the protonation of the tetrapyrrole ring and aggregation of the porphyrin fragments in the film.[30] The IR spectra [see Figure 1(*d*)] revealed a shift of the tetrapyrrole cycle vibrations towards lower frequencies upon the formation of the poly-**3** film, which can be associated with the increase in the substituent effective mass.[31,32] It may indicate the formation of poly-porphyrins linked *via* a lateral substituent. This assumption was confirmed by changes in the bands of out-of-plane collective C–H vibrations of the phenyl substituent in the region from 840 to 650 cm^{-1} [see Figure 1(*d*), curve *1*]. They were practically disappeared in the spectrum of film [see Figure 1(*d*), curve *2*]. In addition, the relative intensity and position of bands about 1600 cm^{-1} (C=C oscillations of the phenyl ring) were significantly varied. The shoulder at 1735 cm^{-1} was assigned to vibrations of the C=O group, which belongs apparently to the quinoid side or the end groups of the electropolymer formed. The C–O–C bridges act as the main moiety for porphyrin bonding in the electropolymer, and their presence is confirmed by the band at 1123 cm^{-1}.[33–35] The coordination bonds of the central ion can serve as an additional means of the porphyrin bonding in the film. It can be indicated by the appearance of the band at 460 cm^{-1}, which is presumably attributed to the vibrations of the Zn–O bond.[36,37] The halo in the region of 1100 cm^{-1} indicates an incorporation of ClO_4^- ions into the film.[38]

The semiconductor properties of films formed on the Pt electrode were estimated using to the Mott–Schottky approach (see Online Supplementary Materials for details), which revealed a hole type of conductivity of the obtained materials. In the case of poly-**3** films, the concentration of charge carriers was in the range of 10^{25}–10^{26} m^{-3}, and the flat band potential (E_{fb}) was 0.39±0.01 V. The value of potential E_{fb} corresponds to the energy equality state between the charges inside the semiconductor and charges on its surface. If $E \geqslant E_{fb}$, a non-activating transfer of charge through the interphase is possible making the material promising for photo- and electrocatalytic applications. All the obtained films have demonstrated the semiconductor properties. The optical band gap of the semiconducting films was determinated *via* Tauc plots[39–41] (see Online Supplementary Materials). The values of the optical band gap of poly-**1**, poly-**2**, poly-**3** and poly-**4** films on the ITO working electrode were 2.78, 2.68, 2.75 and 2.81 eV, respectively.

In conclusion, we have demonstrated that the method of superoxide-assisted electrochemical deposition can be useful for the production of film materials based on hydroxyphenyl porphyrins and their metal complexes. In this case, the C–O–C bridges act as the major moiety for the bonding of porphyrins inside the electropolymer. DMSO used as the medium ensures a sufficiently safe working environment due to its low toxicity and extends the capabilities of electrodeposition in forming coatings with predetermined properties. The polyporphyrin films prepared according to our method possess a hole type of conductivity.

This work was supported in parts by the Russian Foundation for Basic Research (grant no. 17-03-00678 A) and the Russian Science Foundation (grant no. RSF 14-23-00204P). The authors are grateful to the Upper Volga Region Centre of Physico-Chemical Research at the G. A. Krestov Institute of Solution Chemistry of the Russian Academy of Sciences for a technical support.

Online Supplementary Materials

Supplementary data associated with this article can be found in the online version at doi: 10.1016/j.mencom.2019.05.023.

References

1 M. G. Walter, A. B. Rudine and C. C. Wamser, *J. Porphyrins Phthalocyanines*, 2010, **14**, 7.
2 J. Bonin, A. Maurin and M. Robert, *Coord. Chem. Rev*., 2017, **334**, 184.
3 R. Paolesse, S. Nardis, D. Monti, M. Stefanelli and C. Di Natale, *Chem. Rev*., 2017, **117**, 2517.
4 S. M. Kuzmin, S. A. Chulovskaya and V. I. Parfenyuk, *Adv. Colloid Interface Sci*., 2018, **253**, 23.
5 N. Sh. Lebedeva, E. S. Yurina, Yu. A. Gubarev, S. A. Syrbu and N. L. Pechnikova, *Mendeleev Commun*., 2018, **28**, 158.
6 T. L. Blair, J. R. Allen, S. Daunert and L. G. Bachas, *Anal. Chem*., 1993, **65**, 2155.
7 X. Lu, Y. Quan, Z. Xue, B. Wu, H. Qi and D. Liu, *Colloids Surf., B*, 2011, **88**, 396.
8 J. Humphrey and D. Kuciauskas, *J. Phys. Chem. B*, 2004, **108**, 12016.
9 S. P. Koiry, M. E. Celestin, R. Ratnadurai, P. Veerender, C. Majumder, S. Krishnan, E. Stefanakos, Y. Goswami, D. K. Aswal and S. Bhansali, *Appl. Phys. Lett*., 2013, **103**, 033302.
10 A. Ciszewski and G. Milczarek, *J. Electroanal. Chem*., 1996, **413**, 137.
11 M. Janghouri and M. Adineh, *J. Photochem. Photobiol. A*, 2017, **341**, 31.
12 S. M. Kuzmin, S. A. Chulovskaya, O. I. Koifman and V. I. Parfenyuk, *Electrochem. Commun*., 2017, **83**, 28.
13 S. A. Chulovskaya, S. M. Kuzmin and V. I. Parfenyuk, *Mendeleev Commun*., 2017, **27**, 470.
14 I. H. Wasbotten, J. Conradie and A. Ghosh, *J. Phys. Chem. B*, 2003, **107**, 3613.
15 H. Guo, J. Jiang, Y. Shi, Y. Wang, Y. Wang and S. Dong, *J. Phys. Chem. B*, 2006, **110**, 587.
16 S. M. Kuzmin, S. A. Chulovskaya and V. I. Parfenyuk, *J. Porphyrins Phthalocyanines*, 2015, **19**, 1053.
17 S. M. Kuz'min, S. A. Chulovskaya, M. V. Tesakova, A. S. Semeikin and V. I. Parfenyuk, *Makrogeterotsikly/Macroheterocycles*, 2014, **7**, 218 (in Russian).
18 S. M. Kuzmin, S. A. Chulovskaya and V. I. Parfenyuk, *J. Electroanal. Chem*., 2016, **772**, 80.
19 M. V. Tesakova, A. S. Semeikin and V. I. Parfenyuk, *J. Porphyrins Phthalocyanines*, 2015, **19**, 1034.
20 M. V. Tesakova and V. I. Parfenyuk, *Russ. J. Electrochem*., 2017, **53**, 1281 (*Elektrokhimiya*, 2017, **53**, 1450).
21 A. S. Semeikin, O. I. Koifman and B. D. Berezin, *Chem. Heterocycl. Compd*., 1982, **10**, 1046 (*Khim. Geterotsikl. Soedin*., 1982, 1354).
22 A. B. Ormond and H. S. Freeman, *Dyes Pigm*., 2013, **96**, 440.
23 V. D. Rumyantseva, A. S. Gorshkova and A. F. Mironov, *Makrogeterotsikly/Macroheterocycles*, 2013, **6**, 59.
24 M. Rojkiewicz, P. Kuś, P. Kozub and M. Kempa, *Dyes Pigm*., 2013, **99**, 627.
25 D. T. Sawyer and J. L. Roberts, Jr., *J. Electroanal. Chem*., 1966, **12**, 90.
26 T. Fujinaga, K. Isutsy and T. Adachi, *Bull. Chem. Soc. Jpn*., 1969, **42**, 140.
27 M. Khrizanforov, S. Strekalova, V. Khrizanforova, A. Dobrynin, K. Kholin, T. Gryaznova, V. Grinenko, A. Gubaidullin, M. K. Kadirov and Y. Budnikova, *Top. Catal*., 2018, **61**, 1949.
28 R. A. Schmitz, P. A. Liddell, G. Kodis, M. J. Kenney, B. J. Brennan, N. V. Oster, T. A. Moore, A. L. Moore and D. Gust, *Phys. Chem. Chem. Phys*., 2014, **16**, 17569.
29 M. Speck, H. Kurreck and M. O. Senge, *J. Org. Chem*., 2000, 2303.
30 G. De Luca, A. Romeo and L. M. Scolaro, *J. Phys. Chem. B*, 2006, **110**, 14135.
31 S. F. Mason, *J. Chem. Soc*., 1958, 976.
32 N. Zh. Mamardashvili and O. A Golubchikov, *Russ. Chem. Rev*., 2001, **70**, 577 (*Usp. Khim*., 2001, **70**, 656).
33 G. Socrates, *Infrared and Raman Characteristic Group Frequencies: Tables and Charts*, 3rd edn., John Wiley & Sons, New York, 2004.
34 J. Mohan, *Organic Spectroscopy: Principles and Applications*, CRC Press, Boca Raton, FL, 2004.
35 B. C. Smith, *Infrared Spectral Interpretation: A Systematic Approach*, CRC Press, 2018.
36 J. L. Konne and B. O. Christopher, *J. Nanotechnology*, 2017, Article ID 5219850, DOI:10.1155/2017/5219850.
37 C. P. Rezende, J. B. da Silva and N. D. S. Mohallem, *Braz. J. Phys*., 2009, **39**, 248.
38 L. Pejov and V. M. Petrusevski, *J. Phys. Chem. Solids*, 2002, **63**, 1873.
39 J. Tauc, R. Grigorovici and A. Vancu, *Phys. Status Solidi B*, 1966, **15**, 627.
40 E. A. Davis and N. F. Mott, *Philos. Mag. A*, 1970, **22**, 903.
41 O. Stenzel, *The Physics of Thin Film Optical Spectra: An Introduction*, Springer, Berlin, 2005.

Received: 11th September 2018; Com. 18/5689